

# Self-Assembly of Fibers and Nanorings from Disulfide-Linked Helix–Loop–Helix Polypeptides\*\*

Daniel Aili, Feng-I Tai, Karin Enander, Lars Baltzer, and Bo Liedberg\*

Molecular self-assembly and self-organization are highly interesting approaches for the design of novel functional materials and devices.<sup>[1,2]</sup> The diverse properties of designed polypeptides make them very attractive for such purposes as they are very robust and display enormous structural and chemical flexibility,<sup>[3–5]</sup> which allows for controlled assembly into complex nanometer-scale architectures, such as the coiled-coil polypeptide fibers previously described by Kojima et al.<sup>[6]</sup> and Pandya et al.<sup>[7]</sup>

We present herein a set of designed helix–loop–helix polypeptides that spontaneously, as a result of folding, assemble into nanorings and micrometer-long fibers of four-helix bundles. Fibrous structures are important components in numerous naturally occurring materials with many unique and attractive properties, such as spider silk, keratin, and collagen.<sup>[8]</sup> Finding routes to produce synthetic materials with similar properties is therefore highly desirable.

The molecular building blocks used in this study are the two 42-residue synthetic polypeptides JR2EC and JR2KC.<sup>[9–11]</sup> JR2KC is lysine-rich and has a net charge of +11 at neutral pH, while JR2EC has a large number of glutamic acid residues which give the peptide a net charge of –5. The monomers JR2EC and JR2KC are unordered, but fold into helix–loop–helix motifs upon dimerization, as shown schematically in Figure 1a. Folding is induced by the formation of a hydrophobic core constituted by the hydrophobic sides of the amphiphilic helices. At neutral pH, charge–charge interactions favor heterodimerization through the formation of stabilizing salt bridges while preventing the peptides from undergoing homodimerization. The homodimerization of JR2EC can be induced by adjusting the pH value to less than 6 or by the addition of metal ions, such as Zn<sup>2+</sup>, at neutral pH,<sup>[12]</sup> while the homodimerization of JR2KC has been

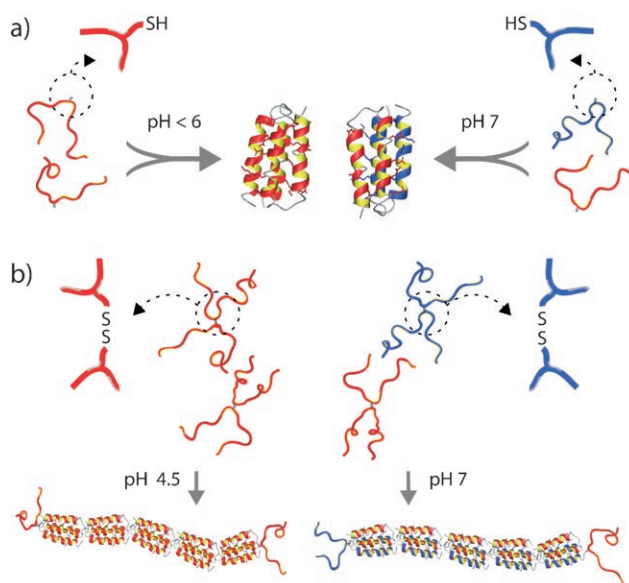


**Figure 1.** a) The two Cys-containing helix–loop–helix polypeptides JR2EC and JR2KC fold into four-helix bundles upon dimerization. Dimerization can be controlled by the pH value. b) When two monomers are linked through a disulfide bridge, the peptides assemble into either homo- or heteroassociated fibers upon folding, depending on the pH value.

observed at pH > 11.<sup>[13]</sup> The dissociation constant ( $K_d$ ) for heterodimerization in solution is 0.02 mM.<sup>[14]</sup>

Both peptides have a Cys residue in position 22, which is located in the loop region. The thiol group of this residue was used to link the monomers through a disulfide bridge into the approximately 9 kDa fiber-forming units (JR2KC)<sub>2</sub> and (JR2EC)<sub>2</sub>. The disulfide-linked monomers were found to spontaneously assemble into long and extremely thin peptide fibers as a result of a propagating association mediated by folding into four-helix bundles (Figure 1b). Fibers were obtained as a result of either heteroassociation (heterofibers) or homoassociation (homofibers), depending on the pH value. To show the importance of folding for fiber formation, an additional peptide was designed with the same primary sequence as JR2EC, but without folding ability. This was achieved by exchanging all the L-Ala residues in JR2EC for D-Ala, while keeping all other amino acids in the L state. The resulting reference peptide, JR2ECref, cannot under any circumstances fold and adopt an ordered secondary structure.<sup>[15]</sup>

Circular dichroism (CD) spectra recorded at pH 7 showed no significant differences in the secondary structure before and after oxidation. The disulfide-linked monomers displayed CD spectra typical for a random-coil arrangement (Figure 2).

[\*] D. Aili, F.-I. Tai, Dr. K. Enander, Prof. B. Liedberg  
Department of Physics, Chemistry and Biology (IFM)  
Linköping University, 58183 Linköping (Sweden)  
Fax: (+46) 13-288-969  
E-mail: bol@ifm.liu.se

Prof. L. Baltzer  
Department of Biochemistry and Organic Chemistry  
Uppsala University, BMC, Box 576, 75123 Uppsala (Sweden)

[\*\*] During this study D.A. and F.-I.T. were enrolled in the graduate school Forum Scientium and in the research programs Biomimetic Materials Science and NanoSense financed by the Swedish Foundation for Strategic Research (S.S.F.). Financial support from the Swedish Research Council (V.R.) and CeNano are also gratefully acknowledged. Many thanks to Daniel Kanmert for valuable discussions.

Supporting information for this article is available on the WWW under <http://dx.doi.org/10.1002/anie.200801155>.

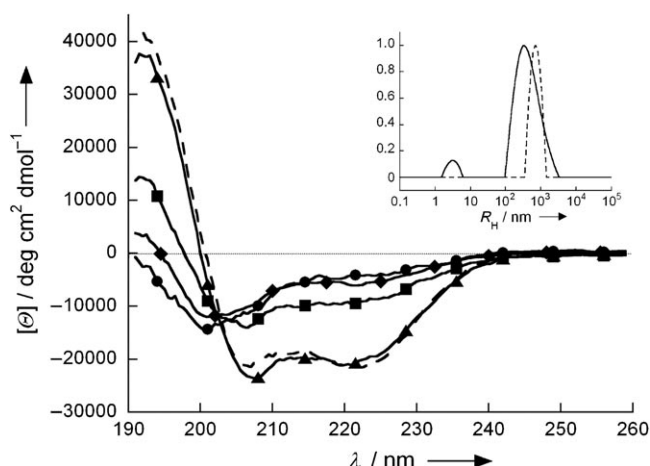


**Figure 2.** CD spectra of the disulfide-linked peptides. At pH 7:  $\blacktriangle$ :  $(\text{JR2KC})_2 + (\text{JR2EC})_2$  (1:1),  $\blacksquare$ :  $(\text{JR2KC})_2 + (\text{JR2ECref})_2$  (1:1),  $\bullet$ :  $(\text{JR2KC})_2$ ,  $\blacklozenge$ :  $(\text{JR2EC})_2$ ; at pH 4.5:  $\blacklozenge$ :  $(\text{JR2EC})_2$ . Inset: Size distribution from DLS studies of: —:  $(\text{JR2KC})_2 + (\text{JR2EC})_2$  (1:1) at pH 7 and  $\cdots$ :  $(\text{JR2EC})_2$  at pH 4.5.

At a 1:1 ratio of  $(\text{JR2KC})_2$  and  $(\text{JR2EC})_2$ , an  $\alpha$ -helical conformation was obtained, with a mean residue ellipticity of  $[\theta]_{222\text{nm}} = (-20.000 \pm 1000) \text{ deg cm}^2 \text{ dmol}^{-1}$ . This value is very similar to those obtained for the folded peptides in the reduced state,<sup>[14]</sup> which suggests that the ability to fold is not significantly altered by oxidation. At pH 4.5,  $(\text{JR2EC})_2$  adopted an  $\alpha$ -helical conformation with a similar helicity as the heteroassociating peptides. No ordered secondary structure was observed when  $(\text{JR2EC})_2$  was replaced by  $(\text{JR2ECref})_2$ .

The hydrodynamic radius ( $R_H$ ) of the fiber-forming units at pH 7 was estimated to be about 3 nm from dynamic light scattering (DLS) studies. When mixing  $(\text{JR2KC})_2$  and  $(\text{JR2EC})_2$  at pH 7 in the presence of 50 mM NaCl, a bimodal size distribution was obtained with one peak corresponding to free fiber-forming units, and one broad peak centered around 420 nm corresponding to the formed fibers (Figure 2, inset). No signs of precipitation were observed under these conditions. Precipitation of heterofibers was, however, observed in the absence of NaCl. Transmission electron microscopy (Figure 3a,b) showed that the heterofibers could reach several micrometers in length. The fiber diameter was about 5 nm, which deviated slightly from the estimated size of the designed four-helix bundle motif (ca.  $2.0 \times 2.5 \text{ nm}$ ) probably as a consequence of the method of staining in combination with the denaturing effect arising from dehydration and adsorption of the fibers on the carbon support material.

Although separated and extended fibers could occasionally be found in the absence of NaCl, fibrous aggregates were often observed when the heterofibers were prepared at low ionic strength (see Figure S1A in the Supporting Information). No fibers or fibrous aggregates could be observed at any salt concentration when using  $(\text{JR2ECref})_2$  instead of  $(\text{JR2EC})_2$ , which strongly suggests that fiber formation requires proper folding. Reducing the concentration of the fiber-forming units from 100 to 25  $\mu\text{M}$  resulted in significantly shorter and more fragmented fibers (see Figure S1B in the Supporting Information). This effect could also be achieved

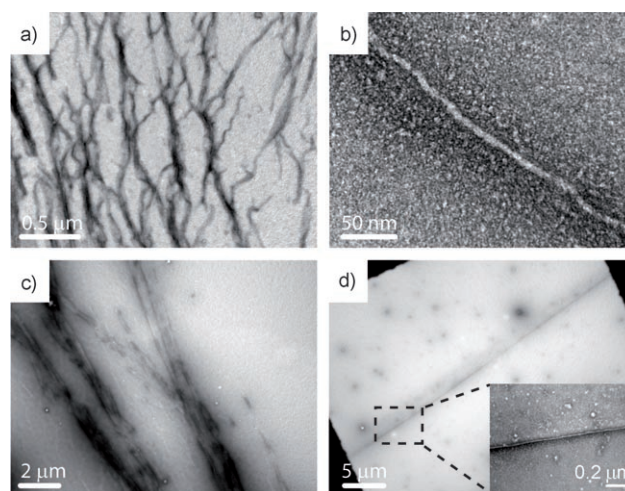


**Figure 3.** a),b) Electron micrographs of fibers formed as a result of heteroassociation of  $(\text{JR2EC})_2$  and  $(\text{JR2KC})_2$  at pH 7. c),d) Fibers formed as a result of homoassociation of  $(\text{JR2EC})_2$  at pH 4.5. The fibers were negatively stained with uranyl acetate and dried on carbon-coated TEM grids.

by capping the fiber ends with a peptide lacking the Cys residue (data not shown).

$(\text{JR2EC})_2$  was found to form extended homofibers at pH 4.5 (Figure 3c,d). The homofibers were in general less aggregated than the heterofibers, probably because of a lower charge attraction between the fibers. Furthermore, the homofibers were typically longer than the heterofibers and could reach approximately 40  $\mu\text{m}$  in length (Figure 3d). DLS studies showed that the homofibers had a size distribution centered at 650 nm (Figure 2, inset). The fibers shown in Figure 3 were prepared by incubating the fiber-forming units for 10 minutes at pH 7 or pH 4.5, which shows that fiber assembly is rapid.

In addition to extended fibers, the heterofibers occasionally assembled into closed loops (nanorings, Figure 4). Ring-like nanostructures have previously been described for a range of polymers and block copolymers,<sup>[16–19]</sup> small organic molecules,<sup>[20]</sup> and inorganic nanoparticles,<sup>[21,22]</sup> and a number of different mechanisms have been proposed to explain the formation of the rings.<sup>[20–24]</sup> The assembly of ringlike structures of polypeptides as a result of folding has, to our knowledge, not been reported before.

The diameter of the rings was in the range of about 400 nm to 5  $\mu\text{m}$ , and rings could be found both in the presence and absence of NaCl at high peptide concentrations (100  $\mu\text{M}$ ). No ring structures were seen at lower peptide concentrations. The fiber length thus seems to be of importance, since longer fibers promote the formation of rings. Aggregated fibers were often observed at and around the rings, particularly in the absence of NaCl. The fibers that organized into rings often appeared less well defined in the electron micrographs and had a slightly larger diameter than the extended fibers. Atomic force microscopy (AFM) height profiles (Figure 4d), however, showed that the ring-forming fibers are only about 1 nm in height when adsorbed on flat silicon surfaces, which suggests that the rings are made either of single fibers or of bundles of fibers that assemble side-by-side. The large size

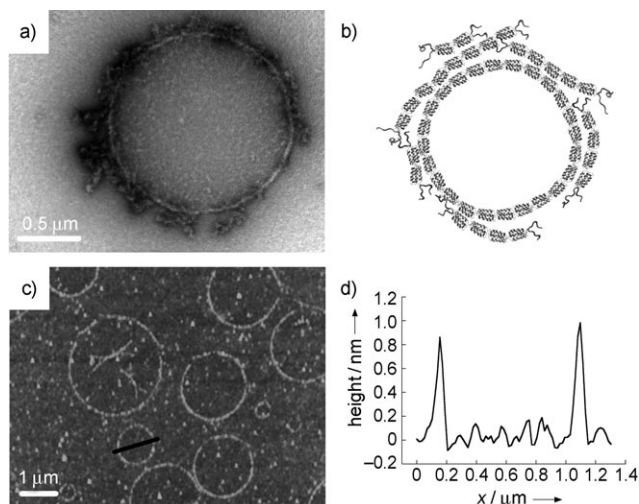


**Figure 4.** a) Electron micrograph of a peptide nanoring stained with uranyl acetate on a carbon-coated TEM grid. b) Schematic representation of the proposed organization of polypeptides into rings. c) AFM topography image of nanorings on a silicon substrate. d) AFM height profile of a nanoring in (c). The black line in (c) indicates the position of the height profile shown in (d).

and high symmetry of the rings, in combination with the apparently larger fiber diameter compared to that of extended fibers, indicate that effects other than just the formation of an intra-supramolecular bond between the fiber ends are involved in the formation of the ring. As water is used as the solvent, ring formation as a result of “breath figures” or Marangoni effects can be excluded, since they require either a phase separation between water and an organic solvent or a more rapid evaporation of the solvent than is possible with water at ambient conditions.<sup>[23,24]</sup> It is more likely that the rings assemble as a result of the formation of holes (2D gas bubbles) that can appear in thin liquid films as the solvent evaporates.<sup>[20,21]</sup> Hole formation has previously been observed for nonvolatile wetting fluids, such as water, and on both wetting and nonwetting surfaces.<sup>[20,21]</sup> The holes are formed to restore the film to its equilibrium thickness when the film becomes unstable because of solvent evaporation.<sup>[25]</sup> Moreover, foreign particles, such as fiber aggregates, may lower the free energy barrier for the formation of 2D bubbles.<sup>[20]</sup> In this case, as the hole grows, fibers and fiber-forming units are forced towards the bulk of the remaining solution and the concentration of the peptides thus increase at the air/water interface, which in turn increases the probability of the formation of fibers and fibrous aggregates that are templated around the hole. The high local concentration of peptides also explains the frequent occurrence of fibrous aggregates around the rings (Figure 4a).

In conclusion, we have described a set of peptides that assemble into fibers of four-helix bundles as a result of folding. The length of the fibers is comparable to peptide fibers reported by other research groups,<sup>[26]</sup> but are considerably smaller in diameter (ca. 5 nm). The rapid and spontaneous folding-driven assembly of peptide fibers and fibrous structures with dimensions at the nanoscale has many potential applications in the area of active biomaterials for, for example, drug delivery and tissue engineering. The

peptide fibers and the fiber-forming units described herein are currently being investigated as new building blocks for a self-assembling nanocomposite previously reported by our research group.<sup>[12,15]</sup>

### Experimental Section

The peptides were synthesized on a solid phase by using a Pioneer automated synthesizer (Applied Biosystems) with standard fluorenylmethoxycarbonyl (Fmoc) chemistry protocols, purified by reversed-phase HPLC, and identified from their MALDI-TOF spectra. Further details on peptide synthesis, amino acid sequences, and experimental details on the characterization of the peptides, fibers, and nanorings can be found in the Supporting Information.

Received: March 10, 2008

Published online: June 23, 2008

**Keywords:** fibers · helical structures · nanostructures · polypeptides · self-assembly

- [1] J.-M. Lehn, *Proc. Natl. Acad. Sci. USA* **2002**, *99*, 4763.
- [2] G. M. Whitesides, B. Grzybowski, *Science* **2002**, *295*, 2418.
- [3] S. G. Zhang, *Nat. Biotechnol.* **2003**, *21*, 1171.
- [4] W. A. Petka, J. L. Harden, K. P. McGrath, D. Wirtz, D. A. Tirrell, *Science* **1998**, *281*, 389.
- [5] A. P. Nowak, V. Breedveld, L. Pakstis, B. Ozbaz, D. J. Pine, D. Pochan, T. J. Deming, *Nature* **2002**, *417*, 424.
- [6] S. Kojima, Y. Kuriki, T. Yoshida, K.-i. Miura, K. Yazaki, *Proc. Jpn. Acad. Ser. B* **1997**, *73*, 7.
- [7] M. J. Pandya, G. M. Spooner, M. Sunde, J. R. Thorpe, A. Rodger, D. N. Woolfson, *Biochemistry* **2000**, *39*, 8728.
- [8] T. Scheibel, *Curr. Opin. Biotechnol.* **2005**, *16*, 427.
- [9] K. P. R. Nilsson, J. Rydberg, L. Baltzer, O. Inganäs, *Proc. Natl. Acad. Sci. USA* **2003**, *100*, 10170.
- [10] S. Olofsson, G. Johansson, L. Baltzer, *J. Chem. Soc. Perkin Trans. 2* **1995**, 2047.
- [11] S. Olofsson, L. Baltzer, *Folding Des.* **1996**, *1*, 347.
- [12] D. Aili, K. Enander, J. Rydberg, I. Nesterenko, F. Björefors, L. Baltzer, B. Liedberg, *J. Am. Chem. Soc.* **2008**, *130*, 5780.
- [13] J. Rydberg, PhD thesis, Linköpings universitet, Linköping, **2006**.
- [14] K. Enander, D. Aili, L. Baltzer, I. Lundström, B. Liedberg, *Langmuir* **2005**, *21*, 2480.
- [15] D. Aili, K. Enander, J. Rydberg, I. Lundström, L. Baltzer, B. Liedberg, *J. Am. Chem. Soc.* **2006**, *128*, 2194.
- [16] Y. M. Gong, Z. J. Hu, Y. Z. Chen, H. Y. Huang, T. B. He, *Langmuir* **2005**, *21*, 11870.
- [17] G. Lu, W. Li, J. M. Yao, G. Zhang, B. Yang, J. C. Shen, *Adv. Mater.* **2002**, *14*, 1049.
- [18] J. K. Kim, E. Lee, Z. G. Huang, M. Lee, *J. Am. Chem. Soc.* **2006**, *128*, 14022.
- [19] I. C. Reynhout, J. J. L. M. Cornelissen, R. J. M. Nolte, *J. Am. Chem. Soc.* **2007**, *129*, 2327.
- [20] A. Schenning, F. B. G. Benneker, H. P. M. Geurts, X. Y. Liu, R. J. M. Nolte, *J. Am. Chem. Soc.* **1996**, *118*, 8549.
- [21] P. C. Ohara, J. R. Heath, W. M. Gelbart, *Angew. Chem.* **1997**, *109*, 1120; *Angew. Chem. Int. Ed. Engl.* **1997**, *36*, 1078.
- [22] B. P. Khanal, E. R. Zubarev, *Angew. Chem.* **2007**, *119*, 2245; *Angew. Chem. Int. Ed.* **2007**, *46*, 2195.
- [23] M. Maillard, L. Motte, A. T. Ngo, M. P. Pileni, *J. Phys. Chem. B* **2000**, *104*, 11871.
- [24] U. H. F. Bunz, *Adv. Mater.* **2006**, *18*, 973.
- [25] F. Brochard-Wyart, J. M. Di Meglio, D. Quere, P. G. De Gennes, *Langmuir* **1991**, *7*, 335.
- [26] D. N. Woolfson, M. G. Ryadnov, *Curr. Opin. Chem. Biol.* **2006**, *10*, 559.